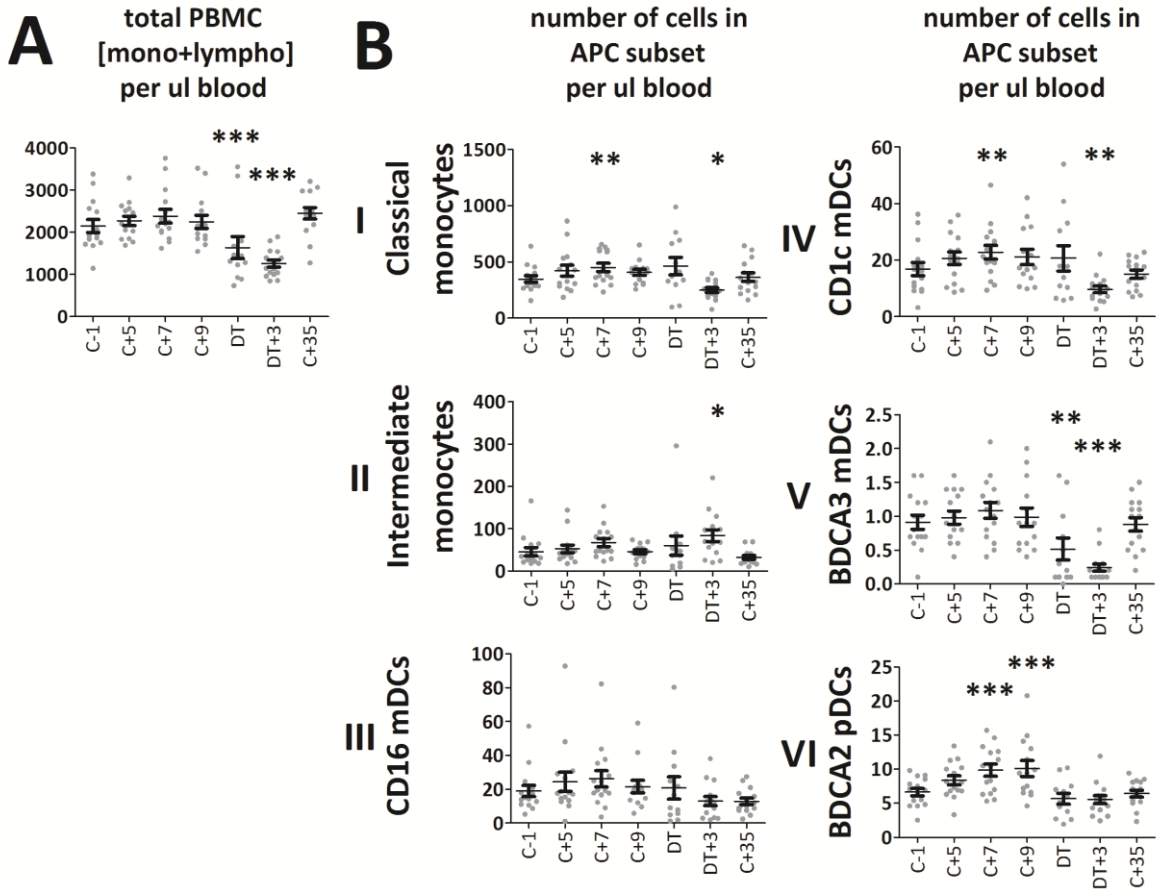




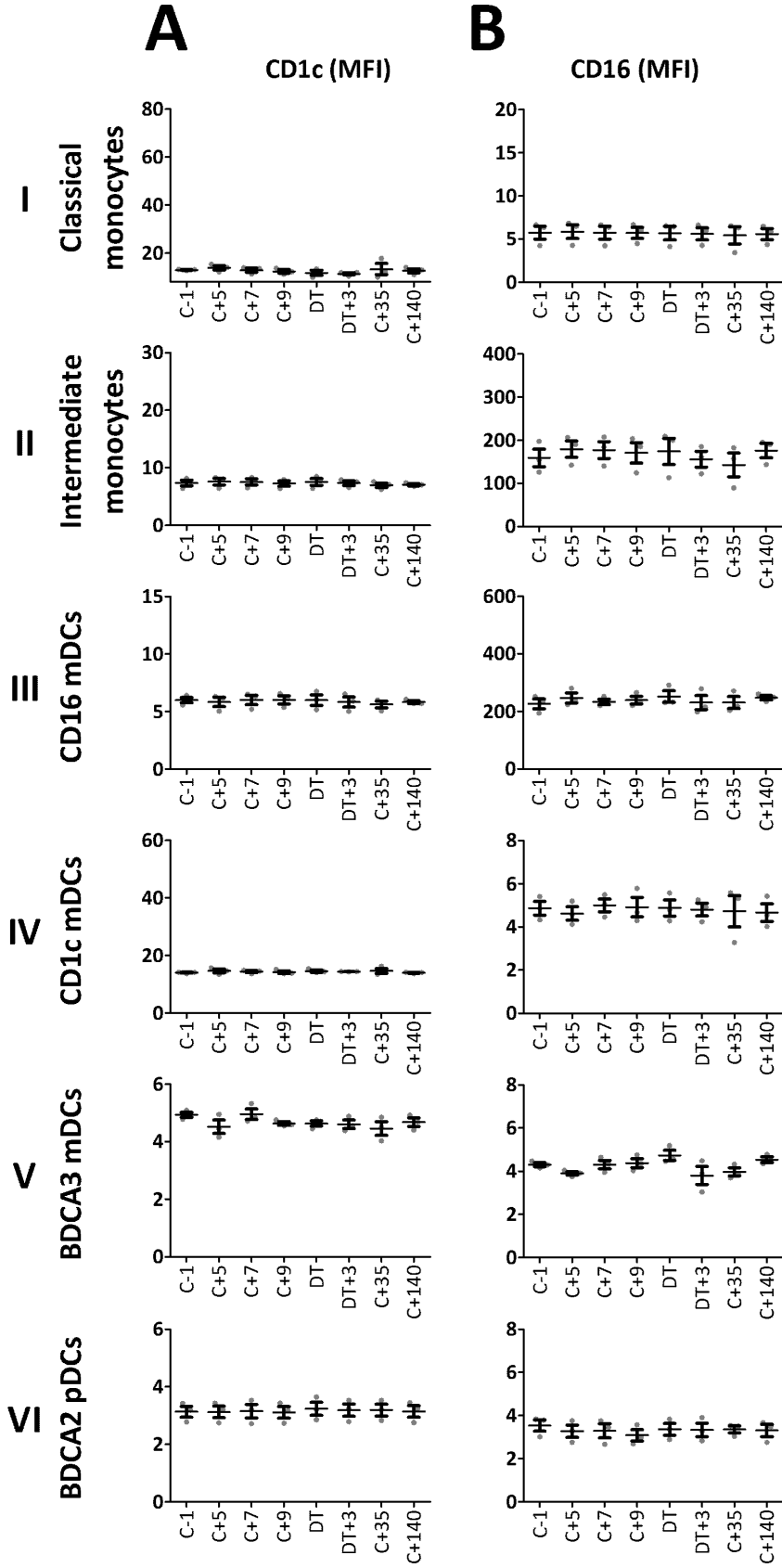
**Figure S1. Kinetics of APC subset frequencies and expression of activation markers during and after CHMI in parasite negative volunteers. (A)** Kinetics of APC subset frequency (% of viable PBMCs). Kinetics of **(B)** HLA-DR expression (geometric mean fluorescence intensity, MFI) and **(C)** CD86 expression (MFI) of the six APC subsets. Data is presented for each individual donor (grey dots) and as mean (n=3) with SEM (black error bars). C, challenge; DT, day of treatment.

Figure S2



**Figure S2. Kinetics of APC subset counts during and after CHMI. (A)** Kinetics of total PBMC counts (adding whole blood counts of lymphocytes and monocytes). **(B)** Kinetics of individual APC subset counts (calculated using whole blood counts and APC subset proportions obtained from flow cytometry data. Data is presented for each individual donor (grey dots) and as mean (n=15 donors that developed parasitaemia after CHMI) with SEM (black error bars). \* p<0.05; \*\* p<0.01; \*\*\* p<0.001, by one-way ANOVA with Dunnet’s posthoc test compared to baseline (C-1). C, challenge; DT, day of treatment.

Figure S3



**Figure S3. CD1c and CD16 expression on APCs during CHMI in parasite negative volunteers.**

Expression (geometric mean fluorescence intensity, MFI) of **(A)** CD1c and **(B)** CD16 on APC subsets over time. Data is presented for each individual donor (grey dots) and as mean (n=3) with SEM (black error bars). C, challenge; DT, day of treatment.